Structural differences and the presence of unsubstituted amino groups in heparan sulphates from different tissues and species

Toshihiko TOIDA*, Hisao YOSHIDA*, Hidenao TOYODA*, Ichiro KOSHIISHI*, Toshio IMANARI*, Ronald E. HILEMAN†, Jonathan R. FROMM† and Robert J. LINHARDT†‡§

*Faculty of Pharmaceutical Sciences, Chiba University, Chiba, Japan, †Division of Medicinal and Natural Products Chemistry, College of Pharmacy, and ‡Department of Chemical and Biochemical Engineering, College of Engineering, University of Iowa, Iowa City, IA 52242, U.S.A.

This study presents a comparison of heparan sulphate chains isolated from various porcine and bovine tissues. ^{1}H-NMR spectroscopy (500 MHz) was applied for structural and compositional studies on intact heparan sulphate chains. After enzymic digestion of heparan sulphate using heparin lyase I (EC 4.2.2.7) II and III (EC 4.2.2.8), the compositions of unsaturated disaccharides obtained were determined by analytical capillary electrophoresis. Correlations between the N-sulphated glucosamine residues and O-sulphation and between iduronic acid content and total sulphation were discovered using the data obtained by NMR and disaccharide analysis. Heparan sulphate chains could be classified into two groups based on the sulphation degree and the iduronic acid content. Heparan sulphate chains with a high degree of sulphation possessed also a significant number of iduronic acid residues and were isolated exclusively from porcine brain, liver and kidney medulla. The presence and amount of N-unsubstituted glucosamine residues (GlcN*p*) was established in all of the heparan sulphates examined. The structural context in which this residue occurs was demonstrated to be: high sulphation domain → 4)-β-D-GlcA*p*-(1 → 4)-α-D-GlcN*p*-(1 → 4)-β-D-GlcA*p*-(1 → low sulphation domain (where GlcN*p* is 2-amino-2-deoxyglucopyranose, and GlcA*p* is glucopyranosyluronic acid), based on the isolation and characterization of a novel, heparin lyase III-derived, GlcN*p* containing tetrasaccharide and hexasaccharide. The results presented suggest that structural differences may play a role in important biological events controlled by heparan sulphate in different tissues.

INTRODUCTION

Heparan sulphate glycosaminoglycan (GAG) is a polydisperse mixture of linear polysaccharides consisting primarily of N-acetylated [→ 4-α-D-GlcN*p*Ac-(1 → 4)-β-D-GlcA*p*-(1 →] and N-sulphated disaccharides [→ 4-α-D-GlcN*p*S-(1 → 4)-β-D-GlcA*p* or -α-L-IdoA*p*-(1 →] that are arranged mainly in segregated domains [1]. Approximately 25 % of the total polymer is formed by alternating arrangements of the two disaccharide units, → 4)-α-D-GlcN*p*S-(1 → 4)-UA*p*-(1 → 4)-α-D-GlcN*p*Ac-(1 → 4)-UA*p*-(1 → 4)-α-D-GlcN*p*S-(1 → . [2]. The polymer is initially synthesized as a repeating → 4)-α-D-GlcN*p*Ac-(1 → 4)-β-D-GlcA*p*-(1 → disaccharide sequence that is attached to a serine residue of a core protein through a tetrasaccharide, glucuronosyl → galactosyl → galactosyl → xylosyl, linkage region [1]. It then undergoes partial N-deacetylation followed by N-sulphation of the newly exposed amino groups, partial C-5 epimerization of D-GlcA*p* to L-IdoA*p* and O-sulphation in a manner similar to the proposed biosynthesis of heparin [3].

Heparan sulphate can usually be easily distinguished from heparin, a related GAG. Heparan sulphate is characterized by a ratio of GlcN*p*Ac to GlcN*p*S of > 3.0, a sulphate content of < 20 %, a D-glucuronic (D-GlcA*p*) to L-iduronic (L-IdoA*p*) acid ratio of > 2, and a carbazole to orcinol ratio of < 2 [4]. Heparan sulphate can show a similarity to heparin in distribution of N-sulphate and N-acetyl groups, but differs in the disposition of O-sulphates and uronic acid epimers [2]. O-Sulphates are always found in proximity to N-sulphates, which enhances the clustering of the sulphate residues and the heterogeneity in chemical composition and charge density of heparan sulphate [5].

Heparan sulphate has a number of important biological activities. Like heparin, heparan sulphate has polysaccharide components that bind antithrombin III [6] and exhibit enhanced specific thrombin-inhibitory and factor-Xa inhibitory activities. Heparan sulphate is involved in cell–cell interaction [7], may function as the endogenous inhibitor of smooth muscle cell proliferation [8] and a regulator of growth factors [9,10], inhibits protease-resistant prion protein accumulation by interfering with the interaction of prion protein with an endogenous GAG or proteoglycan, and may inhibit cell metastasis [11,12] by modulation of cell-surface heparan sulphate content. These and other activities [13] make it a leading target in the development of new pharmaceutical agents such as anti-hypolipemics [14], anti-inflammatories [15], angiogenesis inhibitors [16], anti-dementia agents [17], anticoagulants [13] and anti-arteriosclerotics [18].

Heparan sulphate has been extracted from many different tissues [19]. Intact heparan sulphate has been analysed by high-field NMR [20,21] and following enzymic breakdown [22–29]. The enzymic cleavage of heparan sulphate by heparin lyase I, II and III is stoichiometric, and the cleavage sites are known [22–25,27–29]. These enzymes are eliminases that yield the same non-reducing terminal unsaturated uronic acid residues, ΔUA*p* (4-deoxy-α-L-*threo*-hex-4-enopyranosyluronic acid), from either D-glucuronic acid or L-iduronic acid [30,31].

Abbreviations used: GAG, glycosaminoglycan; GlcN*p*, 2-amino-2-deoxyglucopyranose; IdoA*p*, idopyranosyluronic acid; GlcA*p*, glucopyranosyluronic acid; UA*p*, pyranosyluronic acid; ΔUA*p*, 4-deoxy-α-L-*threo*-hex-4-enopyranosyluronic acid; S, sulphate; Ac, acetyl; CPC, cetylpyridinium chloride; DQF, double-quantum-filtered; TQF, triple-quantum-filtered; COSY, correlation spectroscopy; NOE, nuclear Overhauser effect; 1D, one-dimensional; 2D, two-dimensional; OPA, *o*-phthaldialdehyde; MWCO, M_r cut-off; GPC, gel-permeation chromatography; SAX, strong anion exchange; CE, capillary electrophoresis.

§ To whom correspondence should be addressed, at the College of Pharmacy.

This paper examines a variety of heparan sulphates using chromatographic and chemical methods to study the intact polymer, and capillary electrophoresis and NMR spectroscopy to study enzymically produced oligosaccharides. The results presented suggest the existence of two distinctive and separate populations of heparan sulphates.

EXPERIMENTAL

Materials

Heparin lyase I (heparinase I, EC 4.2.2.7) was from IBEX Technologies (Montreal, Canada). Heparin lyase II (no EC assigned) and heparin lyase III (EC 4.2.2.8) were prepared from *Flavobacterium heparinum* and purified to homogeneity [30]. The disaccharide standards ΔUA*p*2S-(1 → 4)-α-D-GlcN*p*S6S, ΔUA*p*2S-(1 → 4)-α-D-GlcN*p*S, ΔUA*p*-(1 → 4)-α-D-GlcN*p*Ac6S, ΔUA*p*-(1 → 4)-α-D-GlcN*p*S, ΔUA*p*2S-(1 → 4)-α-D-GlcN*p*Ac6S, ΔUA*p*-(1 → 4)-α-D-GlcN*p*Ac6S, ΔUA*p*2S-(1 → 4)-α-D-GlcN*p*Ac and ΔUA*p*-(1 → 4)-α-D-GlcN*p*Ac were from both Sigma Chemical Co. (St. Louis, MO, U.S.A.) and Grampian Enzymes (Aberdeen, U.K.). Chondroitin sulphates from shark cartilage (average M_r 6000, 16000 and 50000, determined by viscometry) were from Seikagaku (Tokyo, Japan). Phosphorus pentoxide, ^2H_2O (99.96%) and 3-trimethylsilyl[$^2H_4$]propionic acid sodium salt were from Aldrich Chemical Co. (Milwaukee, WI, U.S.A.). Capillaries used in electrophoresis were from Dionex (Sunnyvale, CA, U.S.A.) and gel permeation HPLC used an Asahipak column from Asahikasei Co. (Yokohama, Japan). Fluoraldehyde protein/peptide assay solution (*o*-phthaldialdehyde, OPA) was from Pierce, Rockford, IL, U.S.A.

Methods

Preparation of heparan sulphates

Porcine intestinal mucosal heparan sulphate was prepared as previously described [20]. Bovine spleen and pancreas heparan sulphates were generously given by Dr. Bianchinni (Opocrin Research Laboratories, Modena, Italy). Bovine kidney heparan sulphate was from Seikagaku America (Rockville, MD, U.S.A.). Heparan sulphate from porcine brain, lung, pancreas, liver, kidney cortex, kidney medulla and testis were prepared by the following procedure. Wet tissue (200 g) was cut into fine pieces and defatted using a chloroform/methanol [2:1 (v/v), 3.8 litres; 1:1, 2 litres; and 1:2, 2 litres] mixture. Defatted tissue was dried, ground into a very fine powder, treated with Alkalase [32] and β-eliminated with 0.2 M sodium hydroxide containing 50 mM sodium borohydride [33]. Proteins were precipitated with 5% (v/v) perchloric acid and the supernatant was dialysed [M_r cutoff (MWCO) 3000]. Treatment with cetylpyridinium chloride (CPC) gave a precipitate that was recovered by centrifugation and dissolved in 2 M sodium chloride. Methanol precipitation (85%) permitted recovery of pure GAG. Chondroitin lyase ABC treatment (0.2 units in 50 mM sodium acetate, pH 7.4) at 37 °C followed by CPC and methanol precipitation afforded a mixture of heparan sulphate and heparin. The sample was next loaded onto a 30 ml DEAE-Sephadex column in 50 mM Tris acetate, pH 7.4 buffer and eluted stepwise with 0.5 M sodium chloride (heparan sulphate fraction) and 1.5 M sodium chloride (heparin fraction) in the same buffer. Dialysis and freeze-drying afforded between 1.6 and 270 mg of pure heparan sulphate. The heparan sulphate from pancreas contained nucleic acids so it was treated with DNAse [34] and ethanol precipitated.

Estimation of M_r

Samples were dissolved to 1 mg/ml in water and analysed on a Asahipak gel permeation HPLC column at a flow rate of 1 ml/min 50 mM sodium acetate, pH 7.4. Detection was at 206 nm and M_r was estimated using chondroitin and heparan sulphates of average M_r determined by capillary viscometry [20].

^{1}H-NMR analysis

For ^{1}H-NMR spectroscopy, approximately 1 mg of each sample was treated repeatedly three times with 0.5 ml portions of ^2H_2O, followed by desiccation over P_2O_5 *in vacuo* to exchange the labile protons with deuterium. The thoroughly dried sample was redissolved in 0.7 ml of ^2H_2O, and transferred to the NMR tube. All spectra were determined on a Varian UNITY-500 spectrometer at an operating frequency of 500 MHz. The instrument was equipped with a VXR 5000 computer system having a process controller and an array processor. The operation conditions for one-dimensional (1D) spectra were as follows: frequency, 500 MHz; sweep width, 6 kHz; flip angle, 90 (6.6 μs); sampling point, 48k; accumulation, 256 pulses; temperature, 323, 313, 303 and 298 K. Quantitative analysis was performed at each temperature with a pulse delay five times the longest T_1 (5.5 s), estimated from an inversion–recovery experiment. Chemical shifts were indicated by p.p.m. from the signal of 3-trimethylsilyl[$^2H_4$]propionic acid, sodium salt, as an internal standard. A small amount of acetone was used as an internal standard (2.225 p.p.m. at 298 K). The water resonance was suppressed by selective irradiation during the relaxation delay.

Two-dimensional (2D) double-quantum-filtered (DQF), triple-quantum-filtered (TQF) COSY spectra, NOESY and TOCSY spectra were recorded using the phase-sensitive mode. All 2D spectra were recorded with 512 × 1024 data points and a spectral width of 3200 Hz. TOCSY (MLEV-17) spectra were recorded with a mixing time of 100 ms. The water resonance was suppressed by selective irradiation during the relaxation delay. A total of from 128 to 256 scans were accumulated for each t_1, with a relaxation delay of 1.4 s. The digital resolution was 3.2 Hz/point in both dimensions with zero-filling in the t_1

Table 1 Average M_r and content of unsubstituted amino groups in heparan sulphates

–, Not determined.

Sample		Recovery	Average	Unsubstituted amino groups
Species	Tissue	(μg/g of dry tissue)	M_r	(wt% D-GlcN*p*)
Bovine	Kidney	–	10500	1.64
Bovine	Pancreas	–	12500	1.58
Bovine	Spleen	–	12000	1.21
Porcine	Brain	8	11000	3.35
Porcine	Intestine	–	11500†	2.82
Porcine	Kidney cortex	1830	13500	2.32
Porcine	Kidney medulla	1350	10500	2.75
Porcine	Liver	79	12000	2.42
Porcine	Lung	29	9500	5.24
Porcine	Pancreas	43	13000	7.45
Porcine	Testis	129	7000	2.33

†Determined by viscometry and used to calibrate the GPC used for the determination of remaining samples.

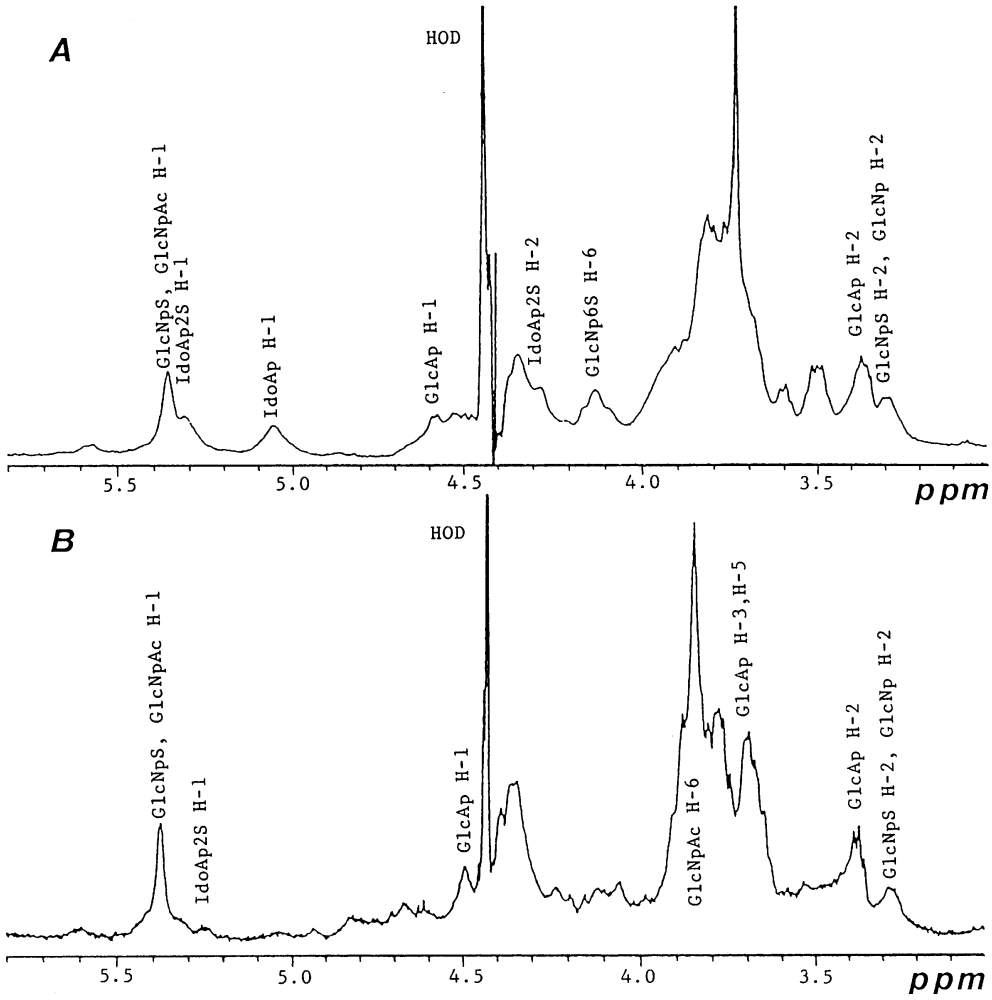

Figure 1 One-dimensional ^{1}H-NMR spectra of heparan sulphates

A representative heparan sulphate with (**A**) high sulphation obtained from porcine kidney medulla and (**B**) low sulphation obtained from porcine kidney cortex.

dimension. A phase-shifted sine function was applied for both t_1 and t_2 dimensions in the case of DQF-COSY, and a Lorentz–Gauss function was applied in all other cases.

Linear baseline correction was applied to all 1D spectra before integral calculations. The relative concentrations of the monosaccharides in each fraction were determined by measuring the integral at their characteristic chemical shifts.

Determination of unsubstituted amino groups

Heparan sulphate samples were assayed for free amino groups by the OPA assay [35] using a procedure supplied with the reagent. Heparan sulphate samples were assayed in triplicate at concentrations that ranged from 10 to 80 μg/ml. Results were compared with a standard curve made from OPA assay of glucosamine at concentrations varying from 0.2 to 2.0 μg/ml to yield mass percent of glucosamine in the individual heparan sulphate samples.

Disaccharide analysis

Each sample was prepared at 10 mg/ml in 50 mM sodium phosphate buffer, pH 7.1 and 100 mM NaCl. The fractions were treated with heparin lyase I, II and III as follows. A small volume addition (1–2 μl) of each lyase (5.6 mU) was added to a vial containing sample in buffer. All of the samples were sealed and incubated for 12 h at 37 °C. The vials were frozen at −20 °C until analysed by capillary electrophoresis.

Preparation of tetrasaccharide and hexasaccharide

A solution was prepared containing 2.5 g of porcine intestinal mucosal heparan sulphate and 2 mg/ml BSA in 100 ml of 50 mM sodium phosphate buffer at pH 7.6. Heparin lyase III (1.25 units) in 20 μl of the same buffer was added to the heparan sulphate substrate solution, and the reactions were incubated at 30 °C until the reaction was complete as measured by absorbance at 232 nm. The oligosaccharide products were concentrated by pressure filtration (10000 MWCO membrane) to remove BSA. The diffusate (510 ml) was collected, freeze-dried, reconstituted in 10 ml of water and fractionated on a Sephadex G-50 (superfine) column (4.8 cm × 1 m) eluted with 200 mM sodium chloride at a flow rate of 2 ml/min. Fractions were collected (10 ml/tube) and absorbance was measured at 232 nm. The fraction numbers were plotted versus absorbance, affording a chromatogram that

showed the separation of disaccharides through octasaccharides. Fractions consisting of tetrasaccharides and hexasaccharides were obtained and evaporated to dryness, desalted by gel permeation chromatography (GPC) on a Bio Gel P-2 column (5 cm × 0.5 m) eluted with water at 6 ml/min and freeze-dried. Charge separation of sized oligosaccharide fractions was carried out by semi-preparative strong-anion exchange (SAX)-HPLC using a linear gradient of sodium chloride at pH 3.5. For example, 30 mg of the desalted tetrasaccharide and hexasaccharide mixtures were injected on a semi-preparative column equilibrated with water at pH 3.5 and eluted using a 120 min gradient from 0.0 to 1.5 M of sodium chloride (pH 3.5) at a flow rate of 4.0 ml/min with monitoring at 232 nm. Peaks that were pure by capillary electrophoresis (CE) analysis were examined for the presence of unsubstituted amino groups. A tetrasaccharide and hexasaccharide were identified, desalted, freeze-dried, and stored at −60 °C. Analytical SAX-HPLC and CE analysis confirmed their purity, and their structure was identified using 2D COSY and NOESY NMR spectroscopy.

Capillary electrophoresis

The experiments were performed on a Dionex capillary electrophoresis system (Sunnyvale, CA, U.S.A.) equipped with a variable-wavelength ultraviolet detector. System operation and data handling were fully controlled using version 3.1 A1-450 chromatography software on an IBM-compatible PC. The CE system was operated in the reverse-polarity mode by applying the sample at the cathode and running using 20 mM phosphoric acid adjusted to pH 3.5 with 1 M dibasic sodium phosphate as previously described [24]. The capillary (75 μm i.d., 375 μm o.d., 77 cm long) was manually washed before use with 0.5 ml of 0.5 M sodium hydroxide, followed by 0.5 ml of distilled water, then 0.5 ml of running buffer. Samples were applied using gravity injection (20 s) by hydrostatic pressure (45 mmHg), resulting in a sample volume of 9.2 nl. Each experiment was conducted at a constant 15000 V. Data collection was at 232 nm. Peaks were identified by co-injection with disaccharide standards.

RESULTS

The porcine heparan sulphates prepared in our laboratory, by a modification of the method of Horner [36], were obtained in yields of 8 to 1830 μg/g dry tissue weight as grey–white powders. The average M_r of these samples, from 7000 to 13500 (Table 1) estimated by GPC, were within the range reported for GAG heparan sulphate [20].

Following exchange with ^2H_2O, the intact heparan sulphate samples were each examined by high-field NMR spectroscopy.

Table 2 Chemical shifts of structural reporter signals of heparan sulphate

–, Not present.

	GlcA	IdoA*p*	Ido2S	GlcN*p*Ac	GlcN*p*Ac6S	GlcN*p*S	GlcN*p*S6S
H-1	4.46	4.99	5.21	5.38	5.39	5.39	5.42
H-2	3.37	3.63	4.34	3.88	3.93	3.32	3.29
H-3	3.58	3.92	4.20	3.85	3.79	3.65	3.64
H-4	3.81	4.15	4.12	3.86	3.79	3.75	3.83
H-5	3.70	4.76	4.79	3.88	4.12	3.75	4.07
H-6a	–	–	–	3.90	4.33	3.8	4.3
H-6b	–	–	–	3.90	4.22	3.8	4.2

Table 3 Monosaccharide composition of heparan sulphates by ^{1}H-NMR analysis

	Hexosamine residue (mol%)		Uronic acid residue (mol%)		
Sample	GlcN*p*Ac	GlcN*p*S	GlcA*p*	IdoA*p*	IdoA*p*2S
Bovine kidney	72.2	27.8	78.2	11.6	10.4
Bovine pancreas	72.5	27.5	75.5	9.4	15.1
Bovine spleen	70.8	20.2	73.3	15.2	11.5
Porcine brain	61.4	38.6	54.6	19.4	26.0
Porcine intestine	72.4	27.6	72.4	6.9	20.7
Porcine kidney cortex	69.2	30.6	73.7	21.8	4.5
Porcine kidney medulla	50.8	48.9	61.6	26.8	11.6
Porcine liver	60.5	39.5	57.9	26.2	15.9
Porcine lung	75.3	24.7	89.5	7.4	3.1
Porcine pancreas	70.2	29.6	86.2	11.8	2.0
Porcine testis	78.6	21.4	74.7	13.6	11.7

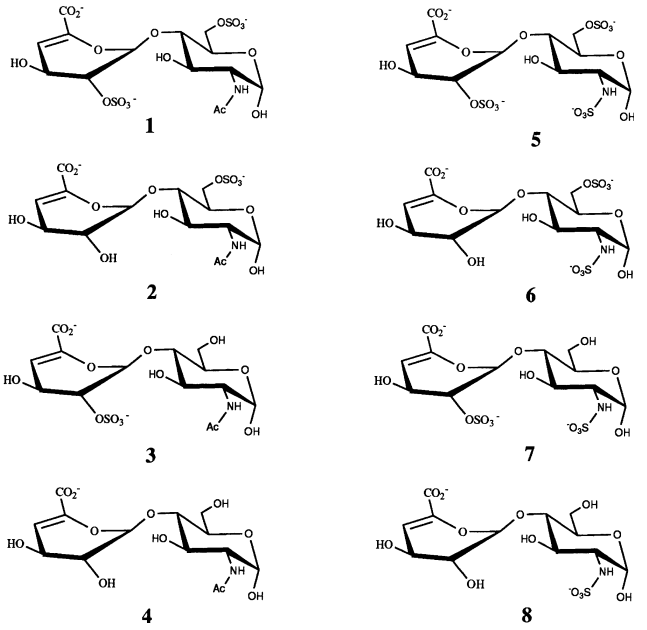

Figure 2 Structure of unsaturated disaccharide standards found in heparan sulphate

Assignments of signals were first made using the 1D spectra (Figure 1) based on reporter signals (Table 2) obtained by the 2D DQF and TQF COSY spectra, TOCSY and nuclear Overhauser effect (NOE) spectra of commercial heparan sulphate from bovine kidney [21]. The anomeric signals of each type of monosaccharide residue were assigned based on their characteristic downfield positions from 4.5 to 5.6 p.p.m. Next, a TOCSY experiment was performed to assign all the ring protons corresponding to the spin system for each monosaccharide residue. Neighbouring protons were assigned by DQF COSY and multiple relayed COSY. Finally, NOE signals were assigned between the anomeric protons and the H-4 protons of the adjacent saccharide residue across the glycosidic linkage to provide sequence connectivities. From these spectra, assignments were made and are presented in Table 2. The 1D spectra of

Table 4 Disaccharide composition of heparan sulphates by capillary electrophoresis analysis

The sulphates/disaccahride values were calculated from the disaccharide composition based on the sulphation level of disaccharides 1–8 (see Figure 2). The ranges of values indicated in the bottom row were observed for the heparan sulphates analysed in this study. n.d., not determined.

Sample	1	2	3	4	5	6	7	8	Sulphates/ disaccharide
Bovine									
Kidney	2.2	12.8	0.0	56.4	1.3	4.2	7.2	15.9	0.60
Pancreas	5.2	10.6	0.0	59.5	1.1	6.6	8.8	8.3	0.63
Spleen	2.4	7.2	0.0	62.8	2.6	4.8	6.5	13.6	0.56
Porcine									
Brain	3.1	7.9	0.0	48.2	12.3	7.3	13.7	7.7	1.01
Intestine	n.d.	4.5	0.0	77.9	< 0.5	1.4	1.1	14.5	0.26
Kidney (cortex)	0.0	10.6	0.0	64.5	3.2	7.5	4.2	9.9	0.54
Kidney (medulla)	0.0	12.1	< 0.5	45.1	15.4	5.4	9.9	12.2	1.01
Liver	0.0	10.2	0.0	47.9	21.2	5.6	4.4	10.8	1.05
Lung	1.6	2.1	0.0	73.4	7.9	1.6	6.3	7.2	0.52
Pancreas	0.0	7.1	0.0	63.4	8.7	3.8	6.1	11.1	0.64
Testis	< 0.5	4.8	0.0	67.5	9.6	2.4	8.1	7.6	0.63
Range	0–5.2	2.1–12.8	0–< 0.5	45.1–77.9	< 0.5–21.2	1.4–7.5	1.1–13.7	7.2–15.9	0.26–1.05

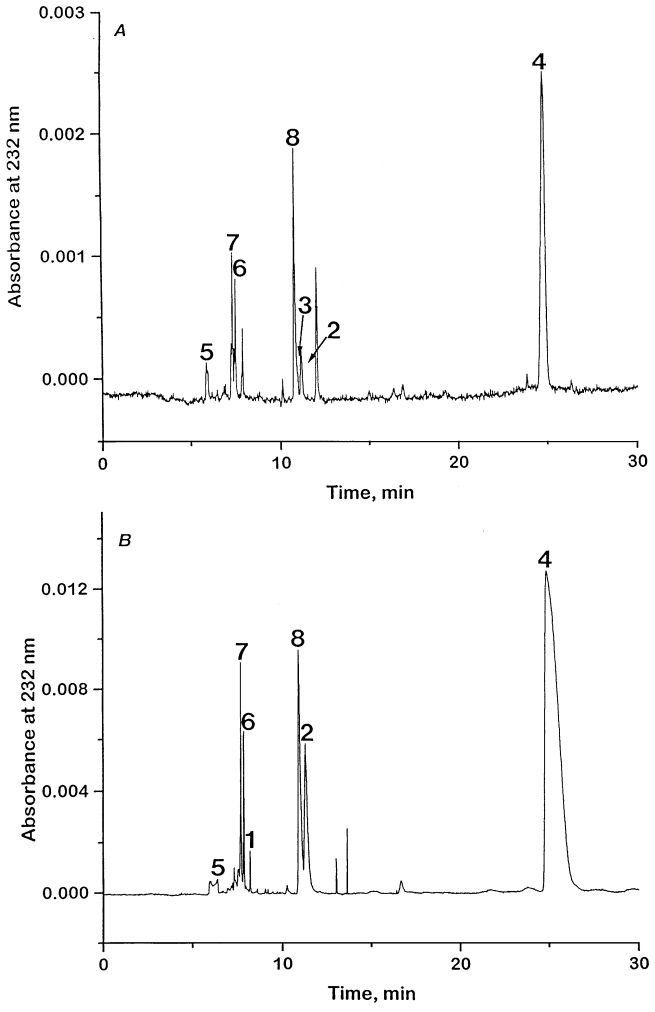

Figure 3 Capillary electropherograms of heparan sulphates treated with an equi-unit mixture of heparin lyases I, II and III

A representative heparan sulphate with (**A**) high sulphation obtained from porcine kidney medulla and (**B**) low sulphation obtained from bovine kidney.

heparan sulphate from porcine kidney medulla and porcine kidney cortex are shown in Figures 1(A) and 1(B) respectively. While both spectra are consistent with heparan sulphate (i.e., a GlcA*p*/IdoA*p* ratio of 2:1), there were significant differences. For example the medullar heparan sulphate contained a substantially higher level of IdoA*p*2S (S = sulphate) than the cortex heparan sulphate, as seen from the intensity of the anomeric signals for this residue at 5.21 p.p.m. (Figures 1A and 1B). The monosaccharide composition, for these and the additional heparan sulphates studied, was determined from the integration of structural reporter signals (Table 2) obtained from their 1D spectra, and are presented in Table 3.

All of the GAG samples used in this study were sensitive to heparin lyase III, confirming that they were indeed heparan sulphates [25,31] (results not shown). Treatment with an equi-unit mixture of heparin lyase I, II and III resulted in nearly complete depolymerization of each sample to disaccharides. Disaccharide analysis using CE relies on a charge-based separation that provides an accurate assessment of the sulphation of a GAG [24]. Using disaccharide standards (Figure 2) nearly all peaks observed on reverse-polarity CE [24] could be identified. The identified disaccharides accounted for $> 90\%$ of the observed peak area. The area under each disaccharide peak was used to obtain the disaccharide composition of each sample (Table 4). From this disaccharide composition the sulphation level of each heparan sulphate was determined. Typical capillary electropherograms of heparin lyase-depolymerized heparan sulphate samples with high and low sulphation are shown in Figure 3.

From these electropherograms it is clear that the predominant unsulphated disaccharide **4** is found in greater amounts in the oligosaccharide map of the heparan sulphate with low sulphation (Figure 3B), whereas the trisulphated disaccharide **5** is found in greater amounts in the heparan sulphate with high sulphation.

Heparan sulphate had previously been shown by other laboratories [37,38] to contain significant amounts of unsubstituted amino groups. The relative amount of unsubstituted amino groups present in each heparan sulphate preparation ranged from 1.2 to 7.5 wt% as determined using OPA (Table 1). Heparan sulphate from porcine intestinal mucosa, which had been previously prepared by our laboratory in gram quantities, contained an average content of unsubstituted amino groups and was used to obtain oligosaccharides from which the structural

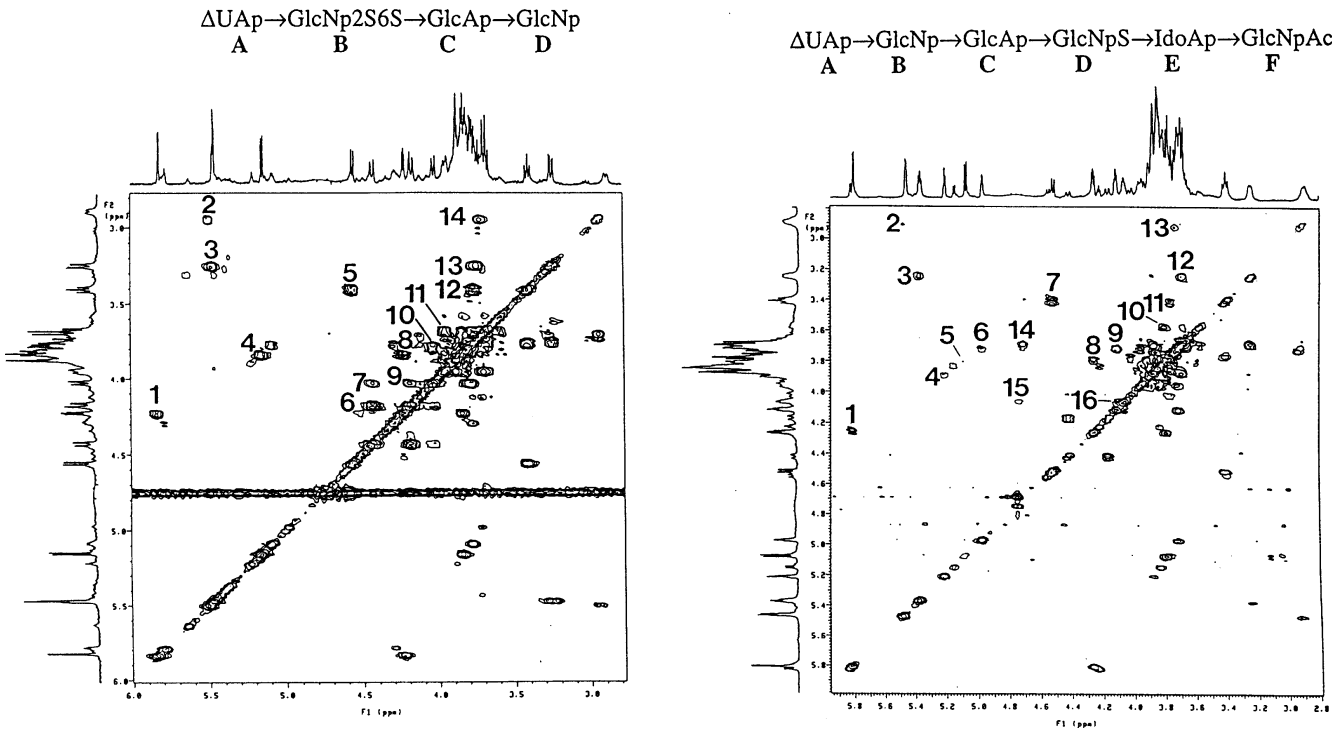

Figure 4 ^{1}H-NMR analyses of heparan sulphate-derived oligosaccharides

Tetrasaccharide 2D COSY spectrum (left panel) cross-peaks are: (1) A3/A4; (2) D1/D2; (3) B1/B2; (4) A1/A2; (5) C1/C2; (6) B6a/B6b; (7) B5/B6a; (8) A2/A3; (9) B5/B6b; (10) B4/B5; (11) D4/D5; (12) C2/C3; (13) B2/B3 and (14) D2/D3. Hexasaccharide 2D COSY spectrum (right panel) cross-peaks are: (1) A3/A4; (2) B1/B2; (3) D1/D2; (4) F1/ F2; (5) A1/A2; (6) E1/E2; (7) C1/C2; (8) A2/A3; (9) E2/E3; (10) F5/F6; (11) C2/C3; (12) D2/D3; (13) B2/B3; (14) F1/F2; (15) E4/E5 and (16) E3/E4.

context of these unsubstituted amino groups could be determined. Complete depolymerization with heparin lyase III followed by size and charge fractionation afforded a tetrasaccharide and a hexasaccharide of $> 90\%$ purity having unsubstituted amino groups. NMR analysis was used to determine the structure of these two oligosaccharides. The 2D COSY spectra of the tetrasaccharide and hexasaccharide are shown in Figure 4. Of particular importance are the cross-peaks (labelled 2 in Figure 4, see legend for cross-peak assignments) between the H-1 and H-2 of the unsubstituted amine containing the GlcN*p* residue. The anomeric proton H-1 of this residue is coupled to a doublet of doublets resonating at 2.9 p.p.m. In the case of the tetrasaccharide the signal at 2.9 p.p.m. integrates as 0.72 protons (in contrast with the one-proton integral for this signal in the hexasaccharide) confirming its presence at a reducing end existing in both α- and β-configurations. This signal at 2.9 p.p.m. and its cross-peak have never been reported in the spectra of other heparin or heparan sulphate oligosaccharides [26–29,39]. The remaining cross-peaks observed in the COSY spectra (Figure 4) in addition to the TOCSY spectra (not shown) confirmed the structure of these two oligosaccharides to be ΔUA*p*-(1 → 4)-α-D-GlcN*p*2S6S(1 → 4)-β-D-GlcA*p*-(1 → 4)-α,β-D-GlcN*p* and ΔUA*p*-(1 → 4)-α-D-GlcN*p*-(1 → 4)-β-D-GlcA*p*-(1 → 4)-α-D-GlcN*p*2S(1 → 4)-α-L-IdoA*p*-(1 → 4)-α,β-D-GlcN*p*Ac (Figure 4).

DISCUSSION

Heparan sulphate is biosynthesized [40] as a proteoglycan and is an ubiquitous component of the extracellular matrix in a wide variety of animal species and tissues [19]. The heparan sulphate proteoglycan consists of a core protein from which one or more GAG side chains extend [1]. The GAG component of heparan sulphate exhibits a wide range of important biological activities [12]. A more highly sulphated but structurally related GAG, heparin, has been used extensively as a pharmacological and therapeutic agent to affect a variety of functions that are regulated endogenously by heparan sulphate [13]. The structure of heparin has been extensively studied by our laboratory [39] and others [29,40–42] because of its therapeutic importance as a major anticoagulant agent [43]. The widespread commercial use of heparin also makes this GAG readily available for structural studies. With the increasing availability of larger, commercial quantities of heparan sulphate [20] the attention of our laboratory has now turned to this important GAG.

Eleven heparan sulphate samples were prepared from a variety of porcine and bovine tissues or obtained from commercial sources. The M_r, NMR spectra, enzymic susceptibility, monosaccharide and disaccharide composition and the sulphate level of these samples varied but were within the range typically observed for heparan sulphates [20].

The monosaccharide composition (Table 3) obtained using NMR spectroscopy of the intact heparan sulphates and the disaccharide composition (Table 4) obtained from the CE of the enzymically depolymerized samples are analysed in Figure 5. The percentage of N-sulphation was first plotted as a function of O-sulphation (Figure 5A). On a similar plot, heparins would cluster between 65 to 98 *N*-sulphates/100 disaccharides and 110 to 180 *O*-sulphates/100 disaccharides (results not shown). Thus, the clear separation between heparan sulphates and heparins

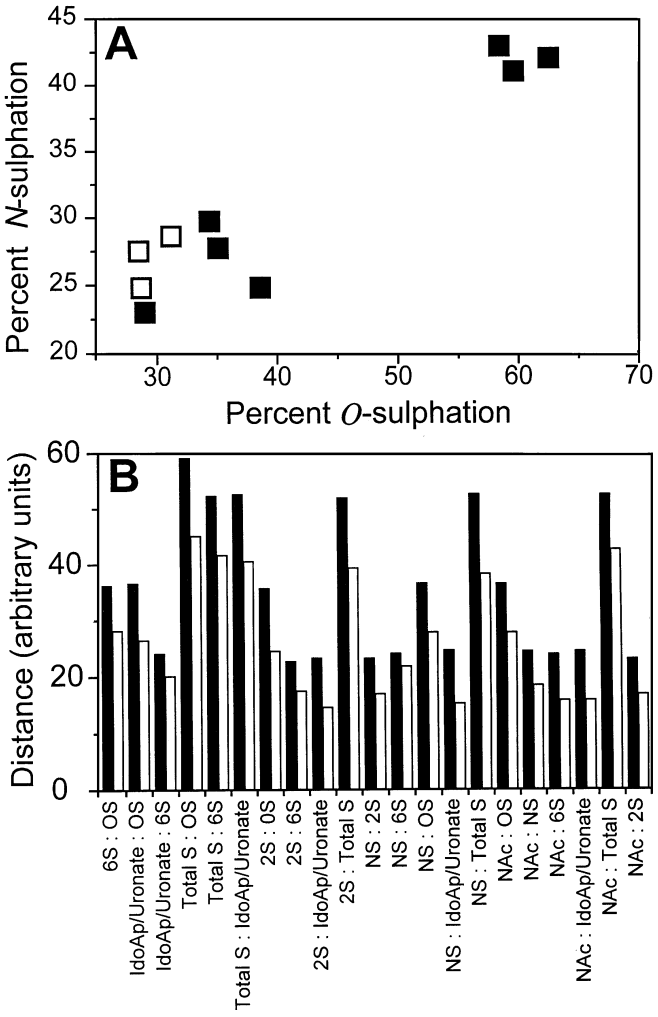

Figure 5 Comparison of structural features of different heparan sulphates and heparins

(**A**) Analysis of compositional data obtained by CE and NMR on heparan sulphates is plotted as percentage of O-sulphation (O-sulphate groups/100 disaccharide units) versus percentage of N-sulphation. Porcine heparan sulphate data are shown with filled squares and bovine heparan sulphate with open squares. (**B**) Analysis of heparan sulphate populations with high sulphation and low sulphation. The methods of comparison shown on the *x*-axis represents a collection of 21 plots of two different structural features. The linear distance in arbitrary units is plotted on the *y*-axis between the centres (filled bars) and the closest point (open bars) between the two discrete populations of heparan sulphates. The data in Table 3 were used to determine the percentage of L-iduronic acid in each sample and the data in Table 4 were used for the percentage of N- and O-sulphation and N-acetylation. Porcine intestinal heparan sulphate was not analysed in Figure 5 since it is prepared using salt fractionation steps to remove heparin [20].

confirms the earlier report of the distinctive nature of the heparan sulphate and heparin family of GAGs [44]. Interestingly, the analysis in Figure 5(A) shows two major populations of heparan sulphates, a highly sulphated species from porcine brain, liver and kidney medulla, the remaining heparan sulphates having lower sulphation. The heparan sulphate population with high sulphation are rich in N- and O-sulphation and contain a high level of L-iduronic acid. While liver heparan sulphate has been previously reported to be highly sulphated due to the presence of heparin-like domains [45], no similar observations have been made regarding brain or kidney medullar heparan sulphates. To more fully analyse the structural features of these two populations of heparan sulphates, 21 plots (similar to the one shown in Figure 5A) were constructed. Each plot corresponded to two different structural properties for each heparan sulphate. In each plot, the same two populations of heparan sulphates were clearly observed. The first corresponding to highly sulphated porcine brain, liver and kidney medulla and the second to the remaining heparan sulphates. The data obtained in these 21 plots are presented graphically in Figure 5(B). In each of the 21 plots the linear distance between the centre point of the two heparan sulphate populations was determined to serve as a measure of how different these populations were. In addition, the closest point between these two populations in each plot was determined as a measure of the overlap between the populations. All 21 methods of comparison showed a separation of heparan sulphate into the same two discrete populations. The greatest distinction between the two heparan sulphate populations is seen in plots of total sulphation as a function of N-acetylation, N-sulphation, 2-O-sulphation, 6-O-sulphation or total O-sulphation. This suggests that total sulphation level correlates best to high levels of N-sulphation, 2-O-sulphation, 6-O-sulphation and that total O-sulphation also correlates well to low levels of N-acetylation. The smallest distinction between the two heparan sulphate populations was observed in the plot of N-sulphation as a function of 6-O-sulphation. This suggests that the level of N-sulphation correlates poorly to the level of 6-O-sulphation. These correlations may have important implications in understanding the biosynthesis of heparan sulphate proteoglycan.

A similar separation of bovine intestinal mucosal heparins into two populations, called slow-moving and fast-moving heparin, has been reported [46,47]. Fast-moving heparin has a lower average M_r (7920) than slow-moving heparin (14900) and a significantly lower level of sulphation (2.12 sulphates/disaccharide) than slow-moving heparin (2.66 sulphates/disaccharide) [47]. Taken together with the data on heparan sulphate, obtained in the present study, these data suggest that a simple classification of sulphated glucosaminoglycan as heparin or heparan sulphate is not sufficient to define their structure. Furthermore, since GAG structure is intimately associated with activity, the differences between heparan sulphates may play a profound role in the biological function of these molecules.

The content of unsubstituted amino groups in these heparan sulphates was also examined because of recent suggestions that heparan sulphate may play a role in L-selectin binding through these groups [37]. The presence of unsubstituted amino groups in heparan sulphate is not an artifact of purification, since N-sulphate groups survive harsher conditions [48] than are routinely used in heparan sulphate preparation. Recently, monoclonal antibodies have detected unsubstituted amino groups in heparan sulphate from rat kidney tissue [38], but the context or sequences in which these unsubstituted amino groups occur were not established. All heparan sulphates examined in this study contained unsubstituted amino groups of 1.2 to 7.5 wt%, corresponding to 1 to 2 residues in each chain (Table 1). While bovine heparan sulphates contained less unsubstituted amino groups than porcine-derived material, these tissues were processed in different laboratories possibly accounting for the observed differences. More interesting were the differences observed between porcine heparan sulphates that were prepared using identical procedures. No correlation was observed between total N- and O-sulphation and levels of unsubstituted amino groups.

The structural context in which unsubstituted amino groups occur within a heparan sulphate chain was next examined. The

structure of two oligosaccharides containing unsubstituted amino groups were characterized as ΔUA*p*-(1 → 4)-α-D-GlcN*p*2S6S(1 → 4)-β-D-GlcA*p*-(1 → 4)-α,β-D-GlcN*p* and ΔUA*p*-(1 → 4)-α-D-GlcN*p*-(1 → 4)-β-D-GlcA*p*-(1 → 4)-α-D-GlcN*p*2S(1 → 4)-α-L-IdoA*p*-(1 → 4)-α,β-D-GlcN*p*Ac. The unsubstituted amine containing the α-D-GlcN*p* residue is framed by a β-D-GlcA*p* on the reducing and non-reducing end (heparin lyase III cuts at β-D-GlcAp to afford ΔUA*p*). The disaccharide sequence to the non-reducing side of the α-D-GlcN*p* residue contains a highly sulphated α-D-GlcN*p*2S6S residue whereas the entire tetrasaccharide sequence to the reducing side of this residue contains only a single sulphate group. These data suggest that the α-D-GlcN*p* residue may reside in a transition sequence between sequences of high and low sulphation. Studies are ongoing to localize more precisely these residues within the heparan sulphate chain.

This research was supported by the National Institutes of Health (GM38060 and HL52622).

REFERENCES

1 Gallagher, J. T., Turnbull, J. E. and Lyon, M. (1992) Int. J. Biochem. **24**, 553–560
2 Gallagher, J. T., Lyon, M. and Steward, W. P. (1986) Biochem. J. **236**, 313–325
3 Lindahl, U., Lidholt, K., Spillmann, D. and Kjellén, L. (1994) Thromb. Res. **75**, 1–32
4 Linker, A. and Hovingh, P. (1973) Carbohydr. Res. **29**, 41–62
5 Gallagher, J. T. (1987) Nature (London) **326**, 136
6 Marcum, J. A. and Rosenberg, R. D. (1984) Biochemistry **23**, 1730–1737
7 Walker, A. and Gallagher, J. T. (1996) Biochem. J. **317**, 871–877
8 Wright, Jr., T. C., Castellot, J. J., Diamond, J. R. and Karnovsky, M. J. (1989) in Heparin, Chemical and Biological Properties, Clinical Applications (Lane, D. A. and Lindahl, U., eds.), pp. 295–316, Edward Arnold, London
9 Walker, A., Turnbull, J. E. and Gallagher, J. T. (1994) J. Biol. Chem. **269**, 931–935
10 McKeehan, W. L. and Kan, M. (1994) Mol. Reprod. Dev. **39**, 69–81
11 Nakajima, M., Irimura, T., Di Ferrante, D., Di Ferrante, N. and Nicolson, G. L. (1983) Science **220**, 611–613
12 Parish, C. R., Coombe, D. R., Jakobsen, J. B., Bennet, F. A. and Underwood, P. A. (1987) Int. J. Cancer **40**, 511–518
13 Linhardt, R. J. and Toida, T. (1997) in Carbohydrates as Drugs (Witczak, Z. B. and Nieforth, K. A., eds.), Marcel Dekker, in the press
14 Engleberg, H. (1984) Pharmacol. Res. **36**, 91–110
15 Nelson, R. M., Venot, A., Bevilacqua, M. P., Linhardt, R. J. and Stamenkovic, I. (1995) Annu. Rev. Cell Dev. Biol. **11**, 601–631
16 Rong, G. H., Alessandri, G. and Sindelar, W. F. (1986) Cancer **57**, 586–590
17 Woods, A. G., Cribbs, D. H., Wittemore, E. R. and Cotman, C. W. (1995) Brain Res. **697**, 53–62
18 Grossman, B. J., Cifonelli, J. A. and Ozoa, A. K. (1971) Atherosclerosis **13**, 103–108
19 Nader, H. B. and Dietrich, C. P. (1989) in Heparin, Chemical and Biochemical Properties, Clinical Applications (Lane, D. A. and Lindah., U., eds.), pp. 81–96, Edward Arnold, London
20 Griffin, C. C., Linhardt, R. J., Van Gorp, C. L., Toida, T., Hileman, R. E., Schubert, R. L. and Brown, S. E. (1995) Carbohydr. Res. **276**, 183–197
21 Toida, T., Qui, G., Matsunaga, T., Sagehashi, Y. and Imanari, T. (1992) Anal. Sci. **8**, 799–804
22 Desai, U. R., Wang, H.-M. and Linhardt, R. J. (1993) Biochemistry **32**, 8140–8145
23 Desai, U. R., Wang, H.-M. and Linhardt, R. J. (1993) Arch. Biochem. Biophys. **306**, 461–468
24 Pervin, A., Al-Hakim, A. and Linhardt, R. J. (1994) Anal. Biochem. **221**, 182–188
25 Linhardt, R. J., Turnbull, J. E., Wang, H. M., Loganathan, D. and Gallagher, J. T. (1990) Biochemistry **29**, 2611–2617
26 Hileman, R. E., Smith, A. E., Toida, T. and Linhardt, R. J. (1997) Glycobiology **7**, in the press
27 Yamada, S., Yoshida, K., Sugiura, M. and Sugahara, K. (1992) J. Biochem. (Tokyo) **112**, 440–447
28 Yamada, S., Yoshida, K., Sugiura, M., Sugahara, K., Khoo, K. H., Morris, H. R. and Dell, A. (1993) J. Biol. Chem. **268**, 4780–4787
29 Yamada, S., Murakami, T., Tsuda, H., Yoshida, K. and Sugahara, K. (1995) J. Biol Chem. **270**, 8696–8705
30 Lohse, D. L. and Linhardt, R. J. (1992) J. Biol. Chem. **267**, 24347–24355
31 Linhardt, R. J. (1994) in Current Protocols in Molecular Biology, Analysis of Glycoconjugates (Varki, A. ed.), vol. 2, pp. 17.13.17–17.13.32, Wiley Interscience, New York
32 Linhardt, R. J., Ampofo, S. A., Fareed, J., Hoppensteadt, D., Mulliken, J. B. and Folkman, J. (1992) Biochemistry **31**, 12441–12445
33 Yanagishita, M. and Hascall, V. C. (1983) J. Biol. Chem. **258**, 12857–12864
34 Furukawa, K. and Terayama, H. (1977) Biochim. Biophys. Acta **499**, 278–289
35 Roth, M. (1971) Anal. Chem. **43**, 880–882
36 Horner, A. A. (1990) Biochem. J. **266**, 553–559
37 Nordgard-Sumnicht, K. and Varki, A. (1995) J. Biol. Chem. **270**, 12012–12024
38 VandenBorn, J., Gunnarsson, K., Bakker, M. A. H., Kjellén, L., Kushe-Gullberg, M., Maccarana, M., Berden, J. H. and Lindahl, U. (1995) J. Biol. Chem. **270**, 31303–31309
39 Pervin, A., Gallo, C., Jandik, K. A., Han, X.-J. and Linhardt, R. J. (1995) Glycobiology **5**, 83–95
40 Lindahl, U., Lidholt, K., Spillman, D. and Kjellén, L. (1994) Thromb. Res. **75**, 1–32
41 Bienkowski, M. J. and Conrad, H. E. (1985) J. Biol. Chem. **260**, 356–365
42 Gettins, P. (1989) Carbohydr. Res. **185**, 69–76
43 Linhardt, R. J. (1991) Chem. Ind. **2**, 45–50
44 Gallagher, J. T. and Walker, A. (1985) Biochem. J. **230**, 665–674
45 Lyon, M., Deakin, J. A. and Gallagher, J. T. (1994) J. Biol. Chem. **269**, 11208–11215
46 Bianchini, P., Osima, B., Parme, B., Nader, H. B., Dietrich, C. P., Casu, B. and Torri, G. (1985) Arzneim. Forsch. **35**, 1215–1219
47 Volpi, N. (1993) Carbohydr. Res. **247**, 263–268
48 Jandik, K. A., Kruep, D., Cartier, M. and Linhardt, R. J. (1996) J. Pharm. Sci. **80**, 45–51

Received 25 July 1996/25 September 1996; accepted 22 October 1996